

Metal–Bosonic Insulator–Superconductor Transition in Boron-Doped Granular Diamond

Gufei Zhang,^{1,*} Monika Zeleznik,² Johan Vanacken,¹ Paul W. May,² and Victor V. Moshchalkov^{1,†}

¹*INPAC-Institute for Nanoscale Physics and Chemistry, KU Leuven, Celestijnenlaan 200D, B-3001 Leuven, Belgium*

²*School of Chemistry, University of Bristol, Bristol BS8 1TS, United Kingdom*

(Received 30 July 2012; published 11 February 2013)

In a variety of superconductors, mostly in two-dimensional (2D) and one-dimensional (1D) systems, the resistive superconducting transition $R(T)$ demonstrates in many cases an anomalous narrow $R(T)$ peak just preceding the onset of the superconducting state $R = 0$ at T_c . The amplitude of this $R(T)$ peak in 1D and 2D systems ranges from a few up to several hundred percent. In three-dimensional (3D) systems, however, the $R(T)$ peak close to T_c is rarely observed, and it reaches only a few percent in amplitude. Here we report on the observation of a giant ($\sim 1600\%$) and very narrow (~ 1 K) resistance peak preceding the onset of superconductivity in heavily boron-doped diamond. This anomalous $R(T)$ peak in a 3D system is interpreted in the framework of an empirical model based on the metal–bosonic insulator–superconductor transitions induced by a granularity-correlated disorder in heavily doped diamond.

DOI: [10.1103/PhysRevLett.110.077001](https://doi.org/10.1103/PhysRevLett.110.077001)

PACS numbers: 74.70.Wz, 71.30.+h, 74.25.-q, 74.62.En

Since the 1950s [1], a puzzling anomalous increase of resistance, $R(T)$, preceding the superconducting transition, has been reported in some superconducting systems situated not yet in the vicinity of the insulator-metal transition (IMT) with relatively low residual resistance. At first, the increase was only observed at the level of a few percent. Later on, in thin films [2–4] and 1D whiskers and wires [5,6], similar effects were also found, with a considerably higher amplitude of the $R(T)$ anomaly: 16% and 160%. With the discovery of quasi-2D cuprates, the $R(T)$ peak around T_c was also reported for these low-dimensional materials, such as NdCeCuO [7], BiSrCaCuO [8,9], and LaSrCuO [10,11], with the peak amplitude reaching 400%–700%. In 2D and 1D microstructures [6,12–16], made from conventional superconducting materials (mostly Al), a narrow resistance peak close to T_c was also observed, with the peak amplitude reaching the 400% level.

Different models were used to explain the nature of the anomalous $R(T)$ peak: normal-metal–superconductor boundaries, disorder and fluctuations, vortex dynamics and Josephson coupling in layered systems, charge imbalance, and competition between superconducting and insulating states in 2D systems [1,2,4,6,8,12–14,16,17].

All these observations of the $R(T)$ peak around T_c and the corresponding models and theories, formulated to explain the corresponding experimental data, are very much linked to the reduced dimensionality of the investigated systems: 2D or/and 1D. We have found reports on the $R(T)$ peak for 3D-like metallic Cu-Zr glasses only in a couple of previous publications [17,18] with a quite small $R(T)$ peak amplitude—less than 3%. We present here our novel observations of the giant $R(T)$ peak in 3D boron-doped granular diamond, which are very different from previously reported data in the following important aspects.

First, the effect has a giant amplitude: the peak resistance value exceeds the residual resistance close to T_c by 550%–1600%, which is a much higher value than reported before for any system, particularly 2 to 3 orders of magnitude higher (550%–1600%) than previously reported values ($\sim 1\%$ – 3% [17,18]) for any disordered 3D metallic glass.

Second, the giant $R(T)$ peak is observed in heavily boron-doped polycrystalline diamond thick films that are clearly in the 3D regime.

Third, contrary to the superconductor-insulator transition in 2D systems [19], a very steep $R(T)$ increase in our 3D samples is quickly turned into the superconducting transition at lower temperatures [Fig. 1(a)], thus leaving for the emerging giant resistance peak a very narrow temperature window of about 1.7–3.6 K. The observed giant $R(T)$ peak can be interpreted as a result of a sequence of transitions: metal–bosonic insulator–superconductor as temperature goes down. First, localized bosonic islands of Cooper pairs are formed [Fig. 1(b), panel (2)], causing a sharp increase in resistance. At slightly lower temperatures, percolation through these islands, increasing in size, sets in leading to the resistance drop down to zero [Fig. 1(b), panels (3) and (4)].

The polycrystalline diamond thick layers, which we have investigated, were deposited conformally onto the outside of 50- μm -diameter tungsten wires in a specially designed hot filament chemical vapor deposition reactor [20,21]. A gas mixture, 1% CH_4 in H_2 , was thermally dissociated by a hot filament at 2400 K for the growth of undoped diamond (UDD) layers. The high H_2 concentration was employed to etch away sp^2 -carbon impurity phases. Continuous UDD layers with a thickness of ~ 9 – 11 μm were deposited, with the inner tungsten core well covered with no pinholes. To deposit heavily boron-doped diamond (HDD) layers, diborane gas (B_2H_6) diluted in H_2 was added to the gas mixture with a B:C ratio of 1:40.

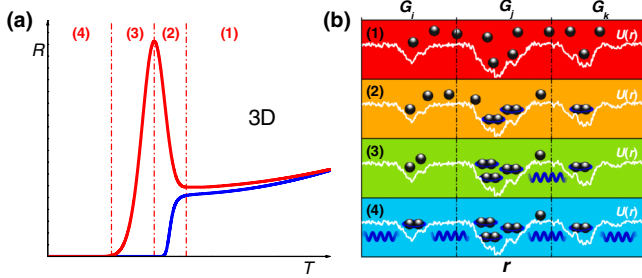


FIG. 1 (color online). Schematic illustration of weak disorder-tuned superconductor-bosonic insulator transition in 3D systems. (a) A disorder-free 3D system undergoes the metal-superconductor transition directly (lower curve), while in many cases a small degree of disorder delays the onset of global superconductivity by tuning the system into a bosonic insulator first. A sequence of transitions [metal-bosonic insulator-superconductor, labeled from (1) to (4) in the figure] gives rise to the anomalous narrow $\rho(T)$ peak just preceding the onset of the global superconducting state $\rho = 0$ at lower temperature (upper curve). (b) Schematic representation of the metal-bosonic insulator-superconductor transition with panels numbered in accordance with Fig. 1(a). Disorder is depicted by spatial variation of the potential $U(r)$; quasiparticles = \bullet ; Cooper pairs = $\bullet\bullet$; G_i , G_j , and G_k = grains on the percolation path; phase locking between bosonic islands = wave curves.

The HDD layers had a thickness of $\sim 3\text{--}5\ \mu\text{m}$, sufficient to form a conformal pinhole-free layer on top of the UDD layers. Scanning electron micrographs showing the granular morphology and the coating structure of the samples can be seen in Fig. 2. The UDD layers were too resistive to measure them with conventional four-probe technique, and hence we measured the current flowing through them

by applying a constant dc voltage of 10 V across two terminals. The $\rho(T)$ dependence so obtained is shown in Fig. 2(e). The negative thermoresistivity observed at 180–270 K in the UDD layers follows Mott’s variable range hopping [inset, Fig. 2(e)] and is typical for conventional insulators. As shown by the scattered data points below 180 K, the current gradually went out of range of the current meter at lower temperatures. The resistivity of the UDD layers is higher than that of the HDD layers by at least 10 orders of magnitude over the whole temperature range 1.9–270 K, which makes the thick UDD layers a very good insulating barrier between the tungsten cores and the HDD layers, ruling out any possibility of current leak due to coexistent conducting channels in tungsten wires and HDD/UDD layers grown on them.

On the highly conductive HDD layers, we performed four-probe ac measurements of the thermoresistivity $\rho(T)$ and magnetoresistivity $\rho(B)$ by using a lock-in amplifier. Figure 2(f) shows the typical $\rho(T)$ behavior of the HDD layers. The resistivity decreases as temperature goes down, and reaches, at around 40 K, a low residual value of $\sim 0.005\text{--}0.009\ \mu\Omega\ \text{m}$, which corresponds to a conductivity about 10^3 times larger than the Mott minimum metallic conductivity $\sim e^2/\hbar a$ (the distance between atoms in diamond $a \sim 1.5\ \text{\AA}$). The residual resistivity is much lower than that of often reported resistivity values of microcrystalline and/or nanocrystalline diamond films [22–25] synthesized with microwave plasma-assisted chemical vapor deposition (MPCVD) method, suggesting good intergrain contacts. Our HDD thick layers were directly deposited on top of the insulating UDD “substrates,” and thus no seeding with undoped nanodiamonds was employed to promote

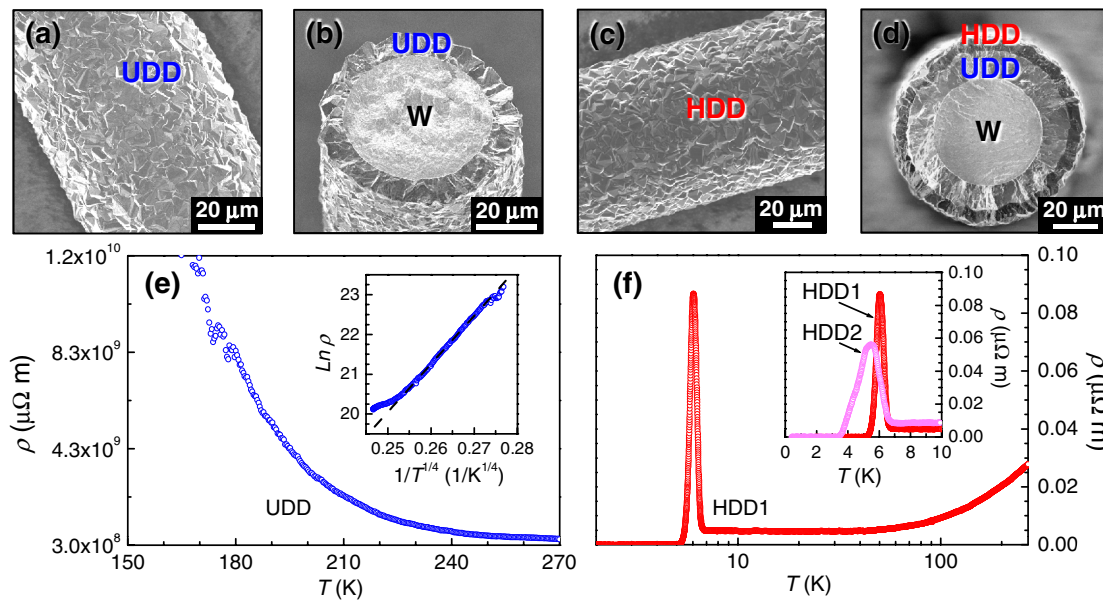


FIG. 2 (color online). Undoped diamond layers and heavily boron-doped diamond layers. Scanning electron micrographs show the granular morphology and the coating structure of our samples. (a) Side view and (b) cross section of UDD layer on a tungsten (W) wire. (c) Side view and (d) cross section of an HDD layer grown on a UDD-coated W wire. Thermoresistivity $\rho(T)$ of UDD (e) and HDD (f) layers.

the diamond nucleation as in MPCVD. Moreover, our samples are a combination of heavy boron doping ($\sim 4 \times 10^{21} \text{ cm}^{-3}$), microscale thickness ($\sim 3\text{--}5 \mu\text{m}$), and big mean grain size ($\sim 6 \mu\text{m}$), which are all crucial in determining the percolative electrical transport of granular diamond systems. When lowering the temperature further, a sharp increase in $\rho(T)$ takes place at about 6.7 K. Within a very narrow temperature window of about 0.7–1.4 K the $\rho(T)$ overshoots the residual resistivity by 550%–1600%, providing a resistivity change per 10 K of about 3800%–23 000% [inset, Fig. 2(f)]. Such a drastic negative thermoresistivity goes far beyond the weak-localization effects where a $d\rho|_{\text{per}10\text{K}} < 10\%$ is normally expected [26], thus indicating the presence of an unconventional insulating state. The large negative thermoresistivity is quickly turned into a sharp resistance decrease accompanying the superconducting transition and the resistivity decreases from the peak value to 0 within a narrow temperature range of $\sim 1.0\text{--}2.2$ K.

To gain an insight into the anomalous $\rho(T)$ peak in the HDD layers, we measured the thermoresistivity $\rho(T)$ in different applied magnetic fields. Figures 3(a) and 3(c) show the behavior of the $\rho(T)$ peak in magnetic fields parallel and perpendicular to the samples, respectively. The applied magnetic field B shifts the whole $\rho(T)$ peak to lower temperatures rather than acting only on the superconducting transition defined from the onset of the zero resistance. Moreover, the height of the $\rho(T)$ peak is systematically and significantly suppressed in higher magnetic fields at lower temperatures. Figures 3(b) and 3(d) present the three-dimensional view of the interpolated data of Figs. 3(a) and 3(c), respectively. In ρ - T - B space, a very large resistivity increase [(“boson insulator” (BI))] looks like a narrow and high “cliff” separating the superconducting (SC) from the metallic state (M). In addition, we do not see any substantial difference between the data measured in a parallel field and in a perpendicular field, suggesting that our samples are in the 3D regime.

The giant resistivity peak preceding the onset of superconductivity was also observed in measurements of magnetoresistivity $\rho(B)$ at different temperatures (not shown). A sufficiently high temperature [> 6.7 K according to the $\rho(T)$ data as shown in Fig. 3] is able to fully recover the metallic nature of the granular HDD layers.

We interpret these observations as follows (see Fig. 4): at $T = T_c$ (local) the superconducting gap opens locally in the grains that together form a 3D system with a small degree of disorder. Granularity-correlated disorder could lead to the localization of individual bosonic droplets (islands of Cooper pairs) [19,27–29] that also absorb the fermions around the Fermi level E_F , thus reducing the normal single quasiparticle conductivity $\sigma_N = 1/\rho_N$. Localized bosonic islands, absorbing “metallic” fermions [Fig. 1(b), panel (2)], are thus responsible for the metal–bosonic insulator transition at T_c (local) with embedded localized superconducting islands [24,25]. With decreasing

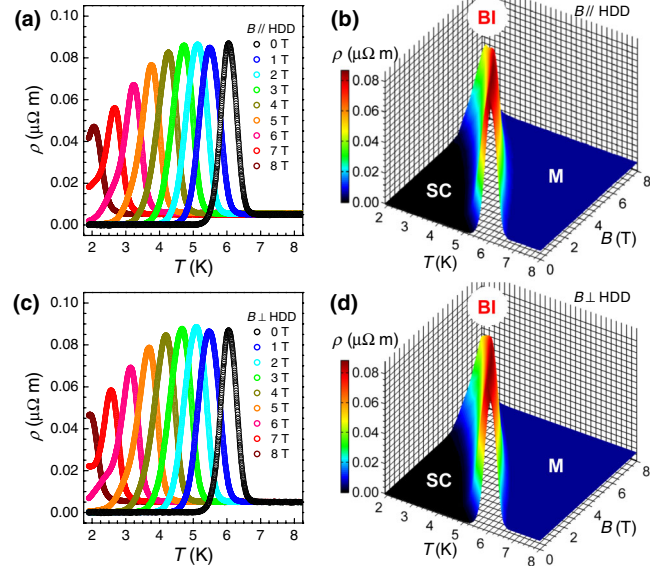


FIG. 3 (color online). The anomalous sharp $\rho(T)$ peak in different applied magnetic fields. (a),(c) The whole $\rho(T)$ peak is shifted and suppressed by magnetic fields (curves from right to left: $0 \rightarrow 8$ T) applied parallel and perpendicular to the samples, respectively. (b), (d) The 3D view of the interpolated data of (a) and (c). The great similarity between data shown in (a), (b) and in (c), (d) suggests that our samples are in the 3D regime. In (b) and (d), M designates metal; BI designates bosonic insulator; and SC designates superconductor.

temperatures bosonic islands continue to grow [Fig. 1(b), panel (3)] and then they start to percolate [Fig. 1(b), panel (4)] in this way providing the onset of global superconductivity at T_c (global). In clean superconductors close to the disorder-free limit [Fig. 4(a)], the two characteristic temperatures are nearly the same: T_c (local) $\sim T_c$ (global), which corresponds to a single and very sharp transition from metallic to superconducting state.

In superconductors with relatively small degree of disorder, as indicated by their very low residual resistance (for example, our 3D doped diamond and Refs. [1–18]), the two characteristic temperatures T_c (local) and T_c (global) are different: T_c (global) $< T_c$ (local). Localized bosonic islands are formed first at higher temperature T_c (local), which leads to the suppression of conductivity $\sigma_N \rightarrow 0$ [Fig. 4(b)] below T_c (local). Contrary to that, the transition at slightly lower temperature $T = T_c$ (global) corresponds to the percolative onset of the zero resistance state, $\rho_S \rightarrow 0$. In strongly disordered superconductors situated in the vicinity of IMT [24,25], the high degree of disorder may result in the formation of localized bosonic islands occurring at different T_c (local), i.e., spatially different T_c (local) [30]. Suppression of conductivity $\sigma_N \rightarrow 0$ is, therefore, a gradual process, giving rise to a bump rather than a sharp peak superimposed within highly resistive background [24,25] preceding the percolative onset of the zero resistance state, $\rho_S \rightarrow 0$. This process leads to a much broader resistive transition with $T_c^{\text{offset}} \ll T_c^{\text{onset}}$.

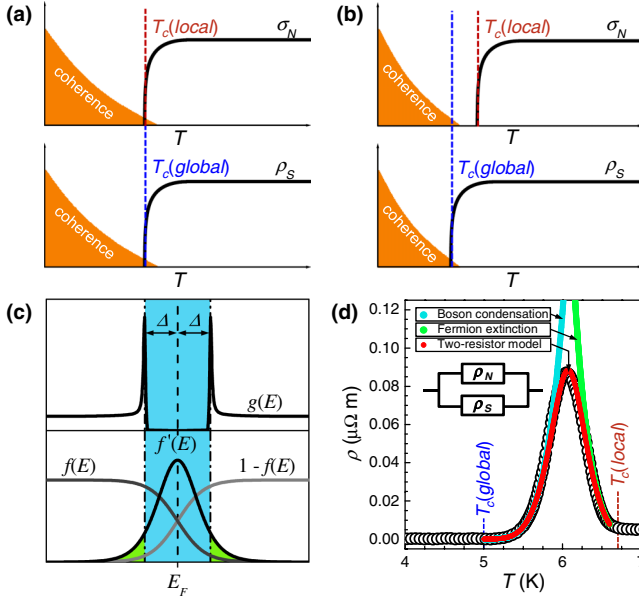


FIG. 4 (color online). Metal–bosonic insulator–superconductor transition modeled by two resistors (normal and superconducting) in parallel. (a) In a disorder-free system, local Cooper pairing and global coherence set in simultaneously, $T_c(\text{local}) = T_c(\text{global})$ and both normal-state conductance, σ_N , and “superconducting” resistance, ρ_S , go to zero at the same temperature. Referring to work by Sacépé *et al.* [28], we highlight the coherence region in orange. (b) In a disordered system, localized bosonic islands are formed at higher temperature $T_c(\text{local})$, leading to the suppression of normal quasiparticle conductivity $\sigma_N \rightarrow 0$. The disorder shifts the percolative onset of zero resistance state $\rho_S \rightarrow 0$ to lower temperature $T_c(\text{global})$. (c) Schematic representation of the removal of quasiparticles from electrical transport by the derivative of the Fermi-Dirac distribution $f'(E)$ filtering the single particle density of states $g(E)$ in the BCS theory. (d) The two-resistor model fitting by Eq. (1) together with the experimental data of the anomalous giant $\rho(T)$ peak. Fermion extinction in the bosonic insulating state is characterized by Eq. (2). Boson condensation is described by Eq. (3).

In a two-resistor (normal and superconducting) model, ρ_N is connected in parallel to ρ_S . Electrical transport can be then approximated as [Fig. 4(d)] [31]

$$\rho_{\text{total}} = \rho_N \rho_S / (\rho_N + \rho_S). \quad (1)$$

The metal–bosonic insulator transition at $T_c(\text{local})$ can be semiempirically modeled as

$$\rho_N(T) = \rho_M \left\{ - \left[2 \int_{\Delta(T)}^{\infty} g(E) f'(E) dE \right] \right\}^{-1}, \quad (2)$$

and the bosonic insulator–superconductor transition at $T_c(\text{global})$ is empirically written as

$$\rho_S(T) = \rho_0 \left[\frac{T}{T_c(\text{global})} - 1 \right]^\eta, \quad (3)$$

where ρ_M is the residual resistivity of the metallic state, and $g(E)$ denotes the single particle density of states in Bardeen-Cooper-Schrieffer (BCS) theory [Fig. 4(c)] [32]:

$$g(E) = \frac{E}{\sqrt{E^2 - \Delta(T)^2}}. \quad (4)$$

Close to $T_c(\text{local})$, we take the parabolic approximation $\tilde{\Delta}(T)$ for $\Delta(T)$,

$$\tilde{\Delta}(T) = \tilde{\Delta}_0 \left[1 - \frac{T}{T_c(\text{local})} \right]^{1/2}, \quad (5)$$

with $\tilde{\Delta}_0$ being the $\tilde{\Delta}(T)$ value extrapolated down to $T=0\text{K}$. Note that $\tilde{\Delta}(T)$ is considerably larger than the BCS value $\Delta(T)$ when $T \ll T_c(\text{local})$, and reaches $\tilde{\Delta}_0 = 1.74 \cdot \Delta(0\text{K})$ at $T=0\text{K}$ [32]. $f'(E)$ is the derivative of the Fermi-Dirac distribution and ρ_0 is left as a fitting parameter.

The proposed simple empirical model describes reasonably well the observed $\rho(T)$ peak [see Fig. 4(d)]. The experimental values of $\rho_M \sim 0.007 \mu\Omega\text{m}$, $T_c(\text{global}) = 5\text{K}$, and $T_c(\text{local}) = 6.7\text{K}$ were adopted, and the following fitting parameters were used: $\rho_0 = 157.4 \mu\Omega\text{m}$, $\eta = 4.8$, and $\tilde{\Delta}_0 = 8.7\text{meV}$. Note that $2\Delta(0\text{K})/k_B T_c = 2\tilde{\Delta}_0/1.74k_B T_c \approx 17$ for our material is relatively high, in accordance with other recently published STM data on a disordered superconductor InO where the observed $2\Delta/k_B T_c$ ratios are in the range of 6.5–11.5 [28], on underdoped $\text{Bi}_2\text{Sr}_2\text{CaCu}_2\text{O}_{8+\delta}$ where $2\Delta(T=83\text{K})/k_B T_c \sim 12.3$ [33], and on overdoped $\text{Bi}_2\text{Sr}_2\text{CuO}_{6+\delta}$ where $2\Delta(T=275\text{mK})/k_B T_c \sim 28$ [34]. We would like also to emphasize that in our case the anomalous giant resistance peak is observed in a 3D system and this makes our experimental findings and the proposed empirical modeling qualitatively different from the well-studied cases with the 1D [5,6,12,14,15] and/or 2D [2–4,7–11,13,16] systems.

Based on the magnetic field dependence of the anomalous giant $\rho(T)$ peak (see Fig. 3), we have constructed the metal–bosonic insulator–superconductor phase diagram as shown in Fig. 5. The magnetic field dependence of $T_c(\text{local})$, $T_c(\text{global})$, and $T(\text{peak})$ divides the H - T space into four regions that are shaded (colored) in accordance with Fig. 1(b). By extrapolating the quadratic fit of the H - $T_c(\text{local})$ phase boundary down to $T=0\text{K}$, we obtain $H(0\text{K}) = 10.8\text{T}$. According to the relation $\xi_{\text{GL}} = [\Phi/2\pi H(0\text{K})]^{1/2}$ with $\Phi = h/2e$ being the flux quantum, we derive the Ginzburg-Landau (GL) coherence length $\xi_{\text{GL}} = 5.5\text{nm}$. This value is quite close to $\xi_{\text{GL}} = 5.3\text{nm}$ determined by using the standard relationship for a dirty type-II superconductor $H(0\text{K}) = -0.69T_c(dH/dT)|_{T_c}$. Note that our $H(0\text{K})$ and ξ_{GL} values are very close to other published data on boron-doped microcrystalline diamond films [22]. With the coherence length of a clean monocrystalline diamond $\xi_0 \sim 15\text{nm}$ [35] and $\xi_{\text{GL}} \sim (l\xi_0)^{1/2}$, the mean free path $l = 1.9\text{nm}$. From $RRR \sim \rho_{270\text{K}}/\rho_{8\text{K}} \sim l/l_{\text{ep}} + 1$, we estimate the electron-phonon scattering length $l_{\text{ep}} = 0.4\text{nm}$.

In conclusion, we have observed a narrow and giant resistance peak preceding the onset of superconductivity in heavily boron-doped polycrystalline diamond situated

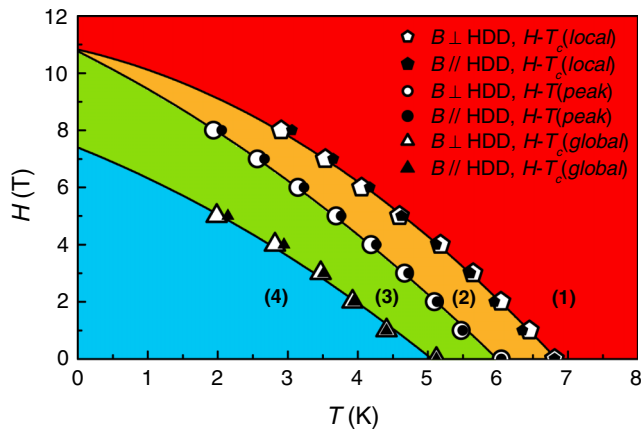


FIG. 5 (color online). Metal-bosonic insulator-superconductor phase diagram colored and numbered in accordance with Fig. 1(b). Based on the magnetic field dependence of the anomalous giant $\rho(T)$ peak, the H - T phase diagram is constructed.

not yet in the vicinity of the IMT. We interpreted these new data in terms of a sequence of transitions (metal-bosonic insulator-superconductor) originating from the formation, in the presence of a small degree of granular disorder, of isolated localized bosonic islands that are efficiently removing fermions from electrical transport and thus strongly enhancing total sample resistance. At slightly lower temperatures, however, an efficient coupling between these bosonic islands sets in and leads to the appearance of global superconductivity with a zero-resistance state.

The work at the KU Leuven is supported by the Methusalem Funding by the Flemish Government and by the FWO projects. M. Z. and P. W. M. thank James Smith for technical assistance and the UK EPSRC for funding.

*Gufei.Zhang@fys.kuleuven.be

†Victor.Moshchalkov@fys.kuleuven.be

- [1] T. G. Berlincourt, *Phys. Rev.* **114**, 969 (1959).
- [2] A. D. C. Grassie and D. B. Green, *Phys. Lett. A* **31**, 135 (1970).
- [3] S. C. Ems and J. C. Swihart, *Phys. Lett. A* **37**, 255 (1971).
- [4] H. Yamamoto, M. Ikeda, and M. Tanaka, *Jpn. J. Appl. Phys.* **24**, L314 (1985).
- [5] Y. Tajima and K. Yamaya, *J. Phys. Soc. Jpn.* **53**, 495 (1984).
- [6] P. Santhanam, C. C. Chi, S. J. Wind, M. J. Brady, and J. J. Bucchignano, *Phys. Rev. Lett.* **66**, 2254 (1991).
- [7] M. A. Crusellas, J. Fontcuberta, and S. Piñol, *Phys. Rev. B* **46**, 14089 (1992).
- [8] Y. M. Wan, S. E. Hebboul, D. C. Harris, and J. C. Garland, *Phys. Rev. Lett.* **71**, 157 (1993).
- [9] E. Silva, M. Lanucara, and R. Marcon, *Physica (Amsterdam)* **276**, 84 (1997).
- [10] M. Suzuki, *Phys. Rev. B* **50**, 6360 (1994).
- [11] C. Buzea, T. Tachiki, K. Nakajima, and T. Yamashita, *IEEE Trans. Appl. Supercond.* **11**, 3655 (2001).
- [12] V. V. Moshchalkov, L. Gielen, G. Neuttiens, C. Van Haesendonck, and Y. Bruynseraede, *Phys. Rev. B* **49**, 15412 (1994).
- [13] M. Park, M. S. Isaacson, and J. M. Parpia, *Phys. Rev. B* **55**, 9067 (1997).
- [14] C. Strunk, V. Bruyndoncx, C. Van Haesendonck, V. V. Moshchalkov, Y. Bruynseraede, C.-J. Chien, B. Burk, and V. Chandrasekhar, *Phys. Rev. B* **57**, 10854 (1998).
- [15] H. Wang, M. M. Rosario, H. L. Russell, and Y. Liu, *Phys. Rev. B* **75**, 064509 (2007).
- [16] A. Harada, K. Enomoto, T. Yakabe, M. Kimata, H. Satsukawa, K. Hazama, K. Kodama, T. Terashima, and S. Uji, *Phys. Rev. B* **81**, 174501 (2010).
- [17] P. Lindqvist, A. Nordström, and Ö. Rapp, *Phys. Rev. Lett.* **64**, 2941 (1990).
- [18] A. Nordström and Ö. Rapp, *Phys. Rev. B* **45**, 12577 (1992).
- [19] T. I. Baturina, A. Yu. Mironov, V. M. Vinokur, M. R. Baklanov, and C. Strunk, *Phys. Rev. Lett.* **99**, 257003 (2007).
- [20] P. G. Partridge, P. W. May, and M. N. R. Ashfold, *Mater. Sci. Technol.* **10**, 177 (1994).
- [21] P. W. May, C. A. Rego, M. N. R. Ashfold, K. N. Rosser, G. Lu, T. D. Walsh, L. Holt, N. M. Everitt, and P. G. Partridge, *Diam. Relat. Mater.* **4**, 794 (1995).
- [22] Y. Takano, M. Nagao, I. Sakaguchi, M. Tachiki, T. Hatano, K. Kobayashi, H. Umezawa, and H. Kawarada, *Appl. Phys. Lett.* **85**, 2851 (2004).
- [23] S. Mandal, C. Naud, O. A. Williams, E. Bustarret, F. Omnès, P. Rodière, T. Meunier, L. Saminadayar, and C. Bäuerle, *Nanotechnology* **21**, 195303 (2010).
- [24] G. Zhang, J. Vanacken, J. Van de Vondel, W. Decelle, J. Fritzsche, V. V. Moshchalkov, B. L. Willems, S. D. Janssens, K. Haenen, and P. Wagner, *J. Appl. Phys.* **108**, 013904 (2010).
- [25] G. Zhang, S. D. Janssens, J. Vanacken, M. Timmermans, J. Vacík, G. W. Ataklti, W. Decelle, W. Gillijns, B. Goderis, K. Haenen, P. Wagner, and V. V. Moshchalkov, *Phys. Rev. B* **84**, 214517 (2011).
- [26] R. W. Simon, B. J. Dalrymple, D. Van Vechten, W. W. Fuller, and S. A. Wolf, *Phys. Rev. B* **36**, 1962 (1987).
- [27] B. Sacépé, C. Chapelier, T. I. Baturina, V. M. Vinokur, M. R. Baklanov, and M. Sanquer, *Phys. Rev. Lett.* **101**, 157006 (2008).
- [28] B. Sacépé, T. Dubouchet, C. Chapelier, M. Sanquer, M. Ovodina, D. Shahar, M. Feigel'man, and L. Ioffe, *Nat. Phys.* **7**, 239 (2011).
- [29] B. L. Willems, V. H. Dao, J. Vanacken, L. F. Chibotaru, V. V. Moshchalkov, I. Guillamón, H. Suderow, S. Vieira, S. D. Janssens, O. A. Williams, K. Haenen, and P. Wagner, *Phys. Rev. B* **80**, 224518 (2009).
- [30] K. K. Gomes, A. N. Pasupathy, A. Pushp, S. Ono, Y. Ando, and A. Yazdani, *Nature (London)* **447**, 569 (2007).
- [31] A. Yazdani and A. Kapitulnik, *Phys. Rev. Lett.* **74**, 3037 (1995).
- [32] M. Tinkham, *Introduction to Superconductivity* (Dover, New York, 2004), Chap. 3.
- [33] Ch. Renner, B. Revaz, J.-Y. Genoud, K. Kadowaki, and Ø. Fischer, *Phys. Rev. Lett.* **80**, 149 (1998).
- [34] M. Kugler, Ø. Fischer, Ch. Renner, S. Ono, and Y. Ando, *Phys. Rev. Lett.* **86**, 4911 (2001).
- [35] E. Bustarret, J. Kačmarčík, C. Marcenat, E. Gheeraert, C. Cytermann, J. Marcus, and T. Klein, *Phys. Rev. Lett.* **93**, 237005 (2004).